Inorg. Chem. **2006**, *45*, 3949–3957

Construction of 3d–4f Mixed-Metal Complexes Based on a Binuclear Oxovanadium Unit: Synthesis, Crystal Structure, EPR, and Magnetic Properties

Wei Shi, Xiao-Yan Chen, Bin Zhao, Ao Yu, Hai-Bin Song, Peng Cheng,* Hong-Gen Wang, Dai-Zheng Liao, and Shi-Ping Yan

Department of Chemistry, Nankai University, Tianjin 300071, People's Republic of China

Received November 16, 2005

The oxovanadium(IV)–lanthanide(III) heteronuclear complexes, $\{[Ce(H_2O)_7(VO)(TTHA)_{0.5}][(VO)_2(TTHA)]\}\cdot 8H_2O$ (**2**), $[Pr(H_2O)_7(VO)_3(TTHA)_{1.5}]\cdot 10H_2O$ (**3**), and $[Nd(H_2O)_7(VO)_3(TTHA)_{1.5}]\cdot 10H_2O$ (**4**) (H_6TTHA = triethylenetetraaminehexaacetic acid), were prepared based on a binuclear building block of $[(VO)_2(TTHA)]^{2-}$ in $[VO(H_2O)_5][(VO)_2TTHA]\cdot 4H_2O$ (**1**). The X-ray crystallographic studies show that **1** is an ion-pair complex, containing the $[(VO)_2(TTHA)]^{2-}$ unit as a useful building block. Adding the light Ln^{3+} ions to this synthesis system, three new 3d–4f mixed-metal-based complexes were obtained. Although the light lanthanide ions always exhibit similar chemical behavior, the structures of **2**–**4** are not homologous. **2** is exhibited as a one-dimensional coordination polymer, comprising an unusual Ce_2V_2 heterometallic lattice in the chain structure, which is the second report of a oxovanadium(IV)–lanthanide(III) coordination polymer. **3** and **4** are isomorphic, every two of the Ln^{3+} cations linked three $[(VO)_2(TTHA)]^{2-}$ anions, forming an interesting linear octanuclear structure. This kind of heteronuclear linear complex is rather rare, which expands the realm of 3d–4f complexes. Further investigations such as IR spectra, UV–vis spectra, magnetic properties, and EPR spectra were studied, and a detailed discussion is given for this system.

Introduction

The construction of transition−lanthanide (3d−4f) mixed-metal supramolecular compounds attracts much attention from chemists due to their exploitable applications, such as magnetism, molecular sensors, luminescent materials and absorption materials in recent years.[1] Since lanthanide ions provide a large unquenched orbital angular moment and the f−f transition is less influenced by the crystal-field compared to the spin−orbit coupling, diverse magnetic behaviors different from the transition-metal ions were observed.[2] Especially when transition metals are bridged to the lanthanide metals by the bridging ligand, forming so-called 3d−4f complexes, not only the attractive topology structure but also the interesting magnetic behavior appeared, such as single-molecule magnets (SMMs).[3] Up to now, though a number of 3d−4f heteronuclear complexes have been well documented, the design and construction of extended structures of 3d−4f heteronuclear coordination polymers or discrete multinuclear aggregation is still a challenge and is of current interest for chemists.[4−6]

* To whom correspondence should be addressed. E-mail: pcheng@nankai.edu.cn.

(1) (a) Lehn, J.-M. *Supramolecular Chemistry*; VCH: Weinheim, 1995; Chapter 9. (b) Hagrman, P. J.; Hagrman, D.; Zubieta, J. *Angew. Chem., Int. Ed.* **1999**, *38*, 2638. (c) Albrecht, M.; Luta, M.; Spek, A. L.; Koten, G. van, *Nature* **2000**, *406*, 970. (d) Bunzli, J. C. G.; Choppin, G. R. *Lanthanide Probes in Life, Chemical and Earth Sciences*; Elsevier: New York, 1989. (e) Valeur, B. *Molecular Fluorescence: Principles and Applications*; Wiley-VCH: Weinheim, 2001. (f) Plecnik, C. E.; Liu, S. M.; Chen, X. N.; Meyers, E. A.; Shore, S. G. *J. Am. Chem. Soc.* **2004**, *126*, 204. (g) Paulovic, J.; Cimpoesu, F.; Ferbinteanu, M.; Hirao, K. *J. Am. Chem. Soc.* **2004**, *126*, 3321.

(2) Benellim, C.; Gatteschi, D. *Chem. Rev.* **2002**, *102*, 2369.

(3) for example: (a) Osa, S.; Kido, T.; Matsumoto, N.; Re, N.; Pochaba, A.; Mrozinski, J. *J. Am. Chem. Soc.* **2004**, *126*, 420. (b) Zaleski, C. M.; Depperman, E. C.; Kampf, J. W.; Kirk, M. L.; Pecoraro, V. L. *Angew. Chem., Int. Ed.* **2004**, *43*, 3912.

(4) (a) Plecynik, C. E.; Liu, S. M.; Shore, S. G. *Acc. Chem. Res.* **2003**, *36*, 499. (b) Bunzli, J.-C. G.; Piguet, C. *Chem. Rev.* **2002**, *102*, 1897.

(5) (a) Zhao, B.; Cheng, P.; Dai, Y.; Cheng, C.; Liao, D. Z.; Yan, S. P.; Jiang, Z. H.; Wang, G. L. *Angew. Chem., Int. Ed.* **2003**, *42*, 934. (b) Zhao, B.; Cheng, P.; Chen, X. Y.; Cheng, C.; Shi, W.; Liao, D. Z.; Yan, S. P.; Jiang, Z. H. *J. Am. Chem. Soc.* **2004**, *126*, 3012. (c) Zhao, B.; Chen, X. Y.; Cheng, P.; Liao, D. Z.; Yan, S. P.; Jiang, Z. H. *J. Am. Chem. Soc.* **2004**, *126*, 15394. (d) Shi, W.; Chen, X. Y.; Zhao, Y. N.; Zhao, B.; Cheng, P.; Yu, A.; Song, H. B.; Wang, H. G.; Liao, D. Z.; Yan, S. P.; Jiang, Z. H. *Chem. Eur. J.* **2005**, *11*, 5031. (e) Zhao, B.; Gao, H. L.; Chen, X. Y.; Cheng, P.; Shi, W.; Liao, D. Z.; Yan, S. P.; Jiang, Z. H. *Chem. Eur. J.* **2006**, *12*, 149.

(6) (a) Zaworotko, M. J. *Chem Commun.* **2001**, 1. (b) Baggio, R.; Garland M. T.; Moreno, Y.; Peña, O.; Perec, M.; Spodine, E. *J. Chem. Soc., Dalton Trans.* **2000**, 2061.

10.1021/ic051979y CCC: $33.50
Published on Web 04/13/2006

In the transition metals, our interest was given to the coordination chemistry of the 3d metal vanadium for its variable valency, plentiful aggregation state, and especially the interrelated applications in the areas of biochemistry, medicine, and catalysis.[7,8] Recently, we have successfully synthesized several VO−Ln (Ln = Pr, Eu, Gd, Ho, and Yb) heteronuclear complexes[5d] in which a binuclear oxovanadium unit $[(VO)_2(TTHA)]^{2-}$ (H_6TTHA = triethylenetetraamine-hexaacetic acid) acts as secondary building unit (SBU).[9] Though the structure of this anion was already documented with alkali metal cation,[10] its potential coordination ability of the abundant oxygen atoms encourages us to study the coordination chemistry of this anion with lanthanide ions. The previous work shows that the dimensionalities of the VO−Ln heteronuclear complexes vary from discrete to 3D according to the increasing atom radius of the lanthanide ions with decreasing atom number. In this contribution, the binuclear oxovanadium SBU was isolated as a new ion-pair complex $[VO(H_2O)_5][(VO)_2TTHA]\cdot 4H_2O$ (**1**) which shows unusual ferromagnetic behavior. Preparation of this complex helps us to further investigate properties of the VO−Ln complexes by comparing the results of VO−Ln complexes with **1**. Three new heteronuclear oxovanadium(IV)−lanthanide(III) complexes: $\{[Ce(H_2O)_7(VO)(TTHA)_{0.5}][(VO)_2(TTHA)]\}\cdot 8H_2O$ (**2**), $[Pr(H_2O)_7(VO)_3(TTHA)_{1.5}]\cdot 10H_2O$ (**3**), and $[Nd(H_2O)_7(VO)_3(TTHA)_{1.5}]\cdot 10H_2O$ (**4**) were obtained with the raw material of $VO(acac)_2$ or $VO(Ac)_2$ instead of $VOSO_4\cdot 3H_2O$ in our previous studies. To the best of our knowledge, the structure of the complexes formed by H_6TTHA and lanthanide ions had not been studied by X-ray diffraction until 1997,[11] while the heteronuclear complexes or the coordination polymers formed with this ligand remain elusive.[5d]

The X-ray crystallographic studies reveal that **2**−**4** contain the same unit $[(VO)_2(TTHA)]^{2-}$ as the building block, but the structures of **2**−**4** are different: **2** is a one-dimensional (1D) coordination polymer, comprising the 1D chain of $[Ce(H_2O)_7(VO)(TTHA)_{0.5}]_n$ and the counterions of $[(VO)_2(TTHA)]^{2-}$. An interesting heterometallic Ce_2V_2 lattice was linked through the −NCCN− bridges of the $TTHA^{6-}$ ligand, which is seldom observed of this ligand in 3d−4f complexes. Although light lanthanide ions (La, Ce, Pr, and Nd) always exhibit the same chemical behavior, the structures of **3** and **4** are different from that of **2**. Both of **3** and **4** comprise the linear octanuclear unit of $[Ln_2(H_2O)_{14}(VO)_6(TTHA)_3]$, which was rather rare in 3d−4f complexes. The Ln−O and V···Ln distances decrease correspondingly as a result of lanthanide contraction.[12] For further investigation of this system, the magnetic and EPR properties were studied and show interesting results.

Experimental Section

Materials and Physical Techniques. All reagents and solvents employed were commercially available and used as received without further purification. Elemental analysis for C, H, and N was obtained at the Institute of Elemental Organic Chemistry, Nankai University. The FTIR spectra were measured with a Bruker Tensor 27 spectrometer on KBr disks. The UV−vis spectra were measured on a JASCO V-570 spectrophotometer. Variable-temperature magnetic susceptibilities were measured on a Quantum Design MPMS-XL SQUID magnetometer. Diamagnetic corrections were made with Pascal's constants for all the constituent atoms. The EPR spectra were measured on a BRUKER EMX-6/1 EPR spectrometer.

Preparations. $[VO(H_2O)_5][(VO)_2TTHA]\cdot 4H_2O$ (1). A mixture of H_6TTHA (0.124 g, 0.25 mmol), $VOSO_4$ (0.122 g, 0.75 mmol), and H_2O (15 mL) was put in a 20 mL acid digestion bomb and heated at 150 °C for 3 days. The product of blue crystals was collected after washing with water (2 × 5 mL) and diethyl ether (2 × 5 mL). Yield: 55%. Anal. Calcd for $C_{18}H_{42}N_4O_{24}V_3$ (851.38): C, 25.39; H, 4.97; N, 6.58. Found: C, 25.11; H, 4.62; N, 6.97.

$\{[Ce(H_2O)_7(VO)(TTHA)_{0.5}][(VO)_2(TTHA)]\}\cdot 8H_2O$ (2). An aqueous solution of H_6TTHA (0.494 g, 1.0 mmol), $VO(Ac)_2$ (0.093 g, 0.5 mmol), $Ce(NO_3)_3\cdot 6H_2O$ (0.109 g, 0.25 mmol), and H_2O (15 mL) was refluxed for 5 h while stirring, then filtered. The suitable crystals were growing by slow evaporation in ethanol atmosphere. The product was collected after washing with water (2 × 5 mL) and diethyl ether (2 × 5 mL). Yield: 55%. Anal. Calcd for $C_{27}H_{66}CeN_6O_{36}V_3$ (1343.80): C, 24.13; H, 4.95; N, 6.25. Found: C, 24.26; H, 5.05; N, 6.35.

$[Pr(H_2O)_7(VO)_3(TTHA)_{1.5}]\cdot 10H_2O$ (3). A mixture of H_6TTHA (0.494 g, 1.0 mmol), $VO(acac)_2$ (0.267 g, 1.0 mmol), $Pr(ClO_4)_3\cdot 6H_2O$ (0.547 g, 1.0 mmol) and H_2O (15 mL) was put in a 20 mL acid digestion bomb and heated at 150 °C for 3 days. The product was collected after washing with water (2 × 5 mL) and diethyl ether (2 × 5 mL). Yield: 70%. Anal. Calcd for $C_{27}H_{70}N_6O_{38}PrV_3$ (1376.59): C, 23.49; H, 5.11; N, 6.09. Found: C, 23.25; H, 5.17; N, 6.16.

$[Nd(H_2O)_7(VO)_3(TTHA)_{1.5}]\cdot 10H_2O$ (4). A mixture of H_6TTHA (0.494 g, 1.0 mmol), $VO(acac)_2$ (0.267 g, 1.0 mmol), Nd_2O_3 (0.336 g, 1.0 mmol), and H_2O (15 mL) was put in a 20 mL acid digestion bomb and heated at 155 °C for 3 days. The product was collected after washing with water (2 × 5 mL) and diethyl ether (2 × 5 mL). Yield: 72%. Anal. Calcd for $C_{27}H_{70}N_6NdO_{38}V_3$ (1383.95): C, 23.42; H, 5.10; N, 6.07. Found: C, 23.25; H, 5.18; N, 6.17.

Crystal Structure Determination. Crystals of **1**−**4** were mounted on glass fibers. Determination of the unit cell and data collection were performed with Mo Kα radiation ($\lambda = 0.71073$ Å) on a BRUKER SMART 1000 diffractometer equipped with a CCD camera. The $\omega-\varphi$ scan technique was employed. The structures

(7) (a) Rhule, J. T.; Hill, C. L.; Judd, D. A. *Chem. Rev.* **1998**, *98*, 327. (b) Cohen, N.; Halberstam, M.; Shlimovich, P.; Chang, C. J.; Shamoon, H.; Rossetti, L. *J. Clin. Invest.* **1995**, *95*, 2501. (c) Thompson, K. H.; McNeil, J. H.; Orvig, C. *Coord. Chem. Rev.* **1999**, *99*, 2561.

(8) (a) Hirao, T. *Coord. Chem. Rev.* **2003**, *237*, 1, and references therein. (b) Koene, B. E.; Taylor, N. J.; Nazar, L. F. *Angew. Chem., Int. Ed.* **1999**, *38*, 2888. (c) Hou, D.; Hagen, K. S.; Hill, C. L. *J. Am. Chem. Soc.* **1992**, *114*, 5864. (d) Hamilton, E. E.; Fanwick, P. E.; Wilker, J. J. *J. Am. Chem. Soc.* **2002**, *124*, 78. (e) Lin, B. Z.; Liu, S. X. *Chem. Commun.* **2002**, 2126. (f) Manos, M. J.; Tasiopoulos, A. J.; Tolis, E. J.; Lalioti, N.; Woollins, J. D.; Slawin, A. M. Z.; Sigalas, M. P.; Kabanos, T. A. *Chem. Eur. J.* **2003**, *9*, 695. (g) Tasiopoulos, A. J.; Troganis, A. N.; Evangelou, A.; Raptopoulou, C. P.; Terzis, A.; Deligiannakis, Y.; Kabanos, T. A. *Chem. Eur. J.* **1999**, *5*, 910. (h) Wolff, F.; Lorber, C.; Choukroun, R.; Donnadieu, B. *Inorg. Chem.* **2003**, *42*, 7839. (i) Mukherjee, A.; Nethaji, M.; Chakravarty, A. R. *Chem. Commun.* **2003**, 2978.

(9) Eddaoui, M.; Moler D. B.; Li, H.; Chen, B.; Reineke, T. M.; O'Keefee, M.; Yaghi, O. M. *Acc. Chem. Res.* **2001**, *34*, 319.

(10) (a) Jiang, Y. Q.; Xie, Z. X. *Chin. J. Struct. Chem.* **2003**, *22*, 423. (b) Long, L.-S.; Ren, Y.-P.; Huang, R.-B.; Zheng, L.-S.; Ng, S. W. *Acta Crystallogr.* **2003**, *E59*, m456.

(11) Mondry, A.; Starynowicz, P. *Inorg. Chem.* **1997**, *36*, 1176.

(12) (a) Li, X. F.; Liu, W. S.; Guo, Z. J.; Tan, M. Y. *Inorg. Chem.* **2003**, *42*, 8735. (b) Pan, L.; Huang, X. Y.; Li, J.; Wu, Y. G.; Zheng, N. W. *Angew. Chem, Int. Ed.* **2000**, *39*, 527. (c) Mizukami, S.; Houjou, H.; Kanesato, M.; Hiratani, K. *Chem. Eur. J.* **2003**, *9*, 1521.

Table 1. Crystal Data and Structure Refinements for **1**−**4**

	1	**2**	**3**	**4**
formula	$C_{18}H_{42}N_4O_{24}V_3$	$C_{27}H_{66}CeN_6O_{36}V_3$	$C_{27}H_{70}N_6O_{38}PrV_3$	$C_{27}H_{70}N_6NdO_{38}V_3$
fw	851.38	1343.80	1376.59	1383.95
T (K)	293(2)	293(2)	294(2)	294(2)
cryst syst	monoclinic	triclinic	monoclinic	monoclinic
space group	$P2(1)/n$	$P\bar{1}$	$C2/c$	$C2/c$
a (Å)	6.879(2)	13.799(3)	19.811(7)	19.808(5)
b (Å)	21.636(7)	14.070(3)	20.204(7)	20.178(5)
c (Å)	11.043(3)	14.693(3)	26.788(10)	26.795(7)
α (deg)	90	61.892(2)	90	90
β (deg)	95.128(5)	83.132(3)	98.402(5)	98.562(4)
γ (deg)	90	89.212(2)	90	90
V (Å^3)	1637.0(9)	2495.1(9)	10607(7)	10590(5)
Z	2	2	8	8
ρ [g/cm^3]	1.727	1.789	1.724	1.736
μ [mm^{-1}]	0.940	1.550	1.524	1.587
θ (deg)	1.88−26.40	2.03−25.03	1.71−28.01	1.45−26.50
index ranges	$-8 \le h \le 8$ $-26 \le k \le 27$ $-8 \le l \le 13$	$-16 \le h \le 12$ $-16 \le k \le 16$ $-17 \le l \le 17$	$-23 \le h \le 26$ $-21 \le k \le 26$ $-35 \le l \le 33$	$-24 \le h \le 24$ $-12 \le k \le 25$ $-33 \le l \le 31$
reflns collected	9244	13 294	35 403	30 742
independent reflns	3333, $R_{int} = 0.0434$	8669, $R_{int} = 0.0185$	12 752, $R_{int} = 0.0406$	10 901, $R_{int} = 0.0605$
max, min transmission	1.000000, 0.848906	1.000000, 0.669030	1.000000, 0.511850	1.000000, 0.726953
data/restraints/params	3333/13/251	8669/39/667	12752/0/690	10901/0/699
GOF on F^2	1.077	1.070	1.074	1.001
R_1, R_2 [I > 2σ (I)]	0.0474, 0.0862	0.0365, 0.1023	0.0447, 0.1087	0.0437, 0.1202
R_1, R_2 (all data)	0.0764, 0.0945	0.486, 0.1076	0.0677, 0.1173	0.0791, 0.1419
largest diff. peak and hole (e·Å^{-3})	0.416 and −0.916	1.109 and −0.741	1.250 and −1.382	0.887 and −0.734

were solved primarily by direct methods and second by Fourier difference techniques and refined by the full-matrix least-squares method. The computations were performed with the SHELXL-97 program.[13,14] All non-hydrogen atoms were refined anisotropically. The hydrogen atoms were set in calculated positions and refined as riding atoms with a common fixed isotropic thermal parameter. CCDC 232782, 287281, 287282, and 287280 contain the supplementary crystallographic data for complexes **1**−**4**, respectively. These data can be obtained free of charge via www.ccdc.cam.ac.uk/conts/retrieving.html (or from the Cambridge Crystallographic Data Center, 12 Union Road, Cambridge CB2 1EZ, UK; fax: (+44) 1223-336-033; or e-mail: deposit@ccdc.cam.ac.uk).

Results and Discussion

Synthesis. As we know, there are two main synthetic strategies to the construction of heteronuclear compounds: (a) the use of a "binucleating ligand" exhibiting inequivalent coordination sites with respect to the ligand filed or the stereochemistry to react with two different metal ions synchronously and (b) the use of a "ligand complex" involving coordination ability to other metal ions.[15] The common ground of the above two strategies is based on the self-assembly process. The only difference lies in that it is a self-assembly process via a basic build unit (BBU) in strategy (a) and it is a self-assembly process via a secondary building unit (SBU) in strategy (b). In this contribution, the 3d−4f complexes were obtained through self-assembly process with the raw material of oxovanadium salts, H_6-TTHA, and the lanthanide salts.

On the other hand, the bulky, flexible EDTA-type organic compound H_6TTHA was first introduced to the 3d−4f system by us. In the reported polyoxovanadate/metal−ligand systems, organic amines are currently used as structure-directing agent, acting as: (i) a charge compensation (or counterion) and space filling constituent; (ii) a bridging ligand coordinates to another metal sites; and (iii) a ligand directly coordinated to the vanadium skeleton.[8,16] In this contribution, H_6TTHA act as the above three characters (see crystal structures). Our previous studies show that Pr forms a 3D coordination polymer, while in this contribution, it only gives a discrete octanuclear structure. The reason may be both the different ratio of the raw materials and the use of $VO(acac)_2$ instead of $VOSO_4 \cdot 3H_2O$ as raw materials.

Crystal Structures of 1−4. Single-crystal diffraction analyses were performed on selected crystals of the complexes (Table 1). Selected bond lengths and angles are listed in Table 2. Since all of the four complexes comprise the same $[(VO)_2(TTHA)]^{2-}$ anion, the structure of **1** will be discussed in the first instance. As shown in Figure 1, V1-(V2) lies in a distorted octahedral coordination environment with three oxygen atoms (V−O, 1.989(2)−1.999(2) Å) and one nitrogen atom (V1−N1, 2.177(3) Å) from the TTHA anion in the equatorial plane. The terminal oxo atom O7 (V1−O7, 1.610(2) Å) along with N2 (V1−N2, 2.278(3) Å) atom occupies the axial position and forms an O7−V1−N2 angle of 174.14(12)°. The V1 atom is displaced from the

(13) Sheldrick, G. M. *SHELXS 97, Program for the Solution of Crystal Structures*; University of Göttingen: Göttingen, Germany, 1997.
(14) Sheldrick, G. M. *SHELXL 97, Program for the Refinement of Crystal Structures*; University of Göttingen: Göttingen, Germany, 1997.
(15) Ohba, M.; Shiozuka, M.; Matsumoto, N.; Okawa, H. *Bull. Chem. Soc. Jpn.* **1992**, *65*, 1988.
(16) (a) Wang, Y.; Yu, J.; Pan, Q. H.; Du, Y.; Zhou, Y. C.; Xu, R. *Inorg. Chem.* **2004**, *43*, 559. (b) Finn, R.; Zubieta, J. *Chem. Commun.* **2000**, 1321.

Table 2. Selected Bond Lengths (Å) and Angles (deg) for **1**−**4**[a]

Complex **1**

V(1)−O(7)	1.610(2)	V(1)−N(1)	2.177(3)	V(2)−O(8)	1.984(2)
V(1)−O(5)	1.989(2)	V(1)−N(2)	2.278(3)	V(2)−O(8B)	1.984(2)
V(1)−O(1)	1.994(2)	V(2)−O(9)	1.894(3)	V(2)−O(10B)	1.999(3)
V(1)−O(3)	1.999(2)	V(2)−O(9B)	1.894(3)	V(2)−O(10)	1.999(3)
O(7)−V(1)−O(5)	102.25(12)	O(5)−V(1)−N(1)	80.09(10)	N(1)−V(1)−N(2)	79.96(9)
O(7)−V(1)−O(1)	96.67(12)	O(1)−V(1)−N(1)	89.25(10)	O(9)−V(2)−O(8)	90.00(12)
O(5)−V(1)−O(1)	159.66(10)	O(3)−V(1)−N(1)	153.04(10)	O(9)−V(2)−O(8B)	90.00(12)
O(7)−V(1)−O(3)	105.45(11)	O(7)−V(1)−N(2)	174.14(12)	O(8)−V(2)−O(8B)	180.00(17)
O(5)−V(1)−O(3)	87.27(10)	O(5)−V(1)−N(2)	83.60(10)	O(9)−V(2)−O(10B)	89.50(13)
O(1)−V(1)−O(3)	94.90(10)	O(1)−V(1)−N(2)	77.48(9)	O(8)−V(2)−O(10B)	89.92(12)
O(7)−V(1)−N(1)	100.47(11)	O(3)−V(1)−N(2)	75.01(9)		

Complex **2**

Ce(1)−O(20)	2.485(3)	V(1)−O(13)	1.600(3)	V(2)−O(9)	1.997(3)
Ce(1)−O(26)	2.496(3)	V(1)−O(5)	1.971(3)	V(2)−N(3)	2.155(3)
Ce(1)−O(27)	2.516(3)	V(1)−O(3)	2.002(3)	V(2)−N(4)	2.287(3)
Ce(1)−O(23)	2.536(3)	V(1)−O(2)	2.006(3)	V(3)−O(21)	1.597(3)
Ce(1)−O(18A)	2.540(3)	V(1)−N(2)	2.176(3)	V(3)−O(15)	1.989(3)
Ce(1)−O(25)	2.550(3)	V(1)−N(1)	2.287(3)	V(3)−O(19)	1.997(3)
Ce(1)−O(24)	2.552(3)	V(2)−O(14)	1.592(3)	V(3)−O(17)	2.002(3)
Ce(1)−O(28)	2.583(3)	V(2)−O(11)	1.974(3)	V(3)−N(6)	2.140(3)
Ce(1)−O(22)	2.637(3)	V(2)−O(7)	1.996(3)	V(3)−N(5)	2.298(3)
O(20)−Ce(1)−O(26)	133.08(10)	O(26)−Ce(1)−O(25)	69.32(12)	O(25)−Ce(1)−O(28)	118.01(12)
O(20)−Ce(1)−O(27)	80.34(10)	O(20)−Ce(1)−O(24)	138.78(10)	O(24)−Ce(1)−O(28)	137.99(11)
O(26)−Ce(1)−O(27)	92.17(11)	O(26)−Ce(1)−O(24)	75.79(11)	O(20)−Ce(1)−O(22)	67.31(9)
O(20)−Ce(1)−O(23)	88.70(10)	O(25)−Ce(1)−O(24)	66.91(11)	O(26)−Ce(1)−O(22)	132.45(11)
O(26)−Ce(1)−O(23)	70.73(11)	O(20)−Ce(1)−O(28)	64.86(10)	O(24)−Ce(1)−O(22)	71.55(10)
O(20)−Ce(1)−O(25)	142.59(11)	O(23)−Ce(1)−O(28)	74.20(12)	O(28)−Ce(1)−O(22)	117.80(11)
O(13)−V(1)−O(5)	103.10(16)	O(14)−V(2)−O(11)	102.48(19)	O(21)−V(3)−O(15)	103.77(14)
O(13)−V(1)−O(3)	103.73(15)	O(14)−V(2)−O(7)	96.75(18)	O(21)−V(3)−O(19)	104.72(13)
O(13)−V(1)−O(2)	96.65(15)	O(14)−V(2)−O(9)	102.75(16)	O(21)−V(3)−O(17)	93.24(14)
O(5)−V(1)−O(2)	159.36(13)	O(7)−V(2)−O(9)	94.25(13)	O(15)−V(3)−O(17)	162.59(12)
O(3)−V(1)−N(2)	153.02(13)	O(14)−V(2)−N(3)	102.35(16)	O(21)−V(3)−N(6)	101.05(14)
O(2)−V(1)−N(2)	89.47(12)	O(11)−V(2)−N(3)	80.91(13)	O(17)−V(3)−N(6)	92.12(12)
O(5)−V(1)−N(1)	84.22(13)	O(14)−V(2)−N(4)	173.26(18)	O(21)−V(3)−N(5)	169.44(14)
O(2)−V(1)−N(1)	76.19(12)	O(9)−V(2)−N(4)	75.55(12)	O(17)−V(3)−N(5)	76.23(11)
N(2)−V(1)−N(1)	79.74(12)	N(3)−V(2)−N(4)	80.23(12)	N(6)−V(3)−N(5)	80.36(12)

Complex **3**

Pr(1)−O(12)	2.428(3)	V(1)−O(13)	1.601(3)	V(2)−O(11)	2.011(3)
Pr(1)−O(22)	2.458(3)	V(1)−O(5)	1.984(3)	V(2)−N(3)	2.158(3)
Pr(1)−O(24)	2.459(4)	V(1)−O(1)	2.002(3)	V(2)−N(4)	2.289(3)
Pr(1)−O(15)	2.459(3)	V(1)−O(3)	2.008(3)	V(3)−O(21)	1.602(3)
Pr(1)−O(27)	2.487(4)	V(1)−N(2)	2.162(3)	V(3)−O(17)	1.990(3)
Pr(1)−O(28)	2.506(3)	V(1)−N(1)	2.297(3)	V(3)−O(19)	1.992(3)
Pr(1)−O(26)	2.511(3)	V(2)−O(14)	1.600(3)	V(3)−O(16)	2.012(3)
Pr(1)−O(23)	2.574(4)	V(2)−O(7)	1.973(3)	V(3)−N(6)	2.147(3)
Pr(1)−O(25)	2.673(4)	V(2)−O(9)	1.999(3)	V(3)−N(5)	2.302(3)
O(12)−Pr(1)−O(22)	74.62(12)	O(24)−Pr(1)−O(27)	76.57(15)	O(28)−Pr(1)−O(26)	69.23(11)
O(12)−Pr(1)−O(24)	82.38(14)	O(15)−Pr(1)−O(28)	72.78(10)	O(12)−Pr(1)−O(23)	68.23(12)
O(22)−Pr(1)−O(24)	140.61(12)	O(27)−Pr(1)−O(28)	70.53(13)	O(28)−Pr(1)−O(23)	114.67(13)
O(12)−Pr(1)−O(15)	79.61(11)	O(12)−Pr(1)−O(26)	135.79(12)	O(26)−Pr(1)−O(23)	68.67(12)
O(22)−Pr(1)−O(15)	74.68(11)	O(22)−Pr(1)−O(26)	98.00(12)	O(12)−Pr(1)−O(25)	67.61(13)
O(22)−Pr(1)−O(27)	140.77(13)	O(27)−Pr(1)−O(26)	75.64(13)	O(23)−Pr(1)−O(25)	123.71(13)
O(13)−V(1)−O(1)	104.70(14)	O(14)−V(2)−O(7)	103.13(16)	O(21)−V(3)−O(17)	104.52(14)
O(5)−V(1)−O(1)	87.75(11)	O(14)−V(2)−O(11)	96.45(15)	O(17)−V(3)−O(19)	88.94(13)
O(13)−V(1)−O(3)	96.60(14)	O(9)−V(2)−O(11)	92.85(12)	O(17)−V(3)−O(16)	92.36(12)
O(1)−V(1)−O(3)	93.11(11)	O(14)−V(2)−N(3)	101.02(14)	O(19)−V(3)−O(16)	160.45(12)
O(13)−V(1)−N(2)	101.54(14)	O(7)−V(2)−N(3)	80.85(12)	O(21)−V(3)−N(6)	101.12(14)
O(3)−V(1)−N(2)	89.95(12)	O(11)−V(2)−N(3)	90.10(12)	O(16)−V(3)−N(6)	89.99(12)
O(13)−V(1)−N(1)	173.38(14)	O(14)−V(2)−N(4)	173.12(16)	O(21)−V(3)−N(5)	171.84(14)
O(5)−V(1)−N(1)	83.92(11)	O(11)−V(2)−N(4)	76.77(11)	O(19)−V(3)−N(5)	85.60(12)
N(2)−V(1)−N(1)	79.73(11)	N(3)−V(2)−N(4)	80.38(11)	N(6)−V(3)−N(5)	80.41(12)

Complex **4**

Nd(1)−O(12)	2.406(4)	V(1)−O(13)	1.599(3)	V(2)−O(11)	2.006(3)
Nd(1)−O(24)	2.438(4)	V(1)−O(5)	1.981(3)	V(2)−N(3)	2.157(4)
Nd(1)−O(22)	2.443(4)	V(1)−O(1)	1.996(3)	V(2)−N(4)	2.289(4)
Nd(1)−O(15)	2.447(4)	V(1)−O(3)	2.004(3)	V(3)−O(21)	1.596(3)
Nd(1)−O(27)	2.466(4)	V(1)−N(2)	2.162(4)	V(3)−O(19)	1.988(4)
Nd(1)−O(28)	2.494(4)	V(1)−N(1)	2.289(4)	V(3)−O(17)	1.991(3)
Nd(1)−O(26)	2.495(4)	V(2)−O(14)	1.591(4)	V(3)−O(16)	2.011(3)
Nd(1)−O(23)	2.548(4)	V(2)−O(7)	1.972(4)	V(3)−N(6)	2.142(4)
Nd(1)−O(25)	2.678(5)	V(2)−O(9)	1.997(3)	V(3)−N(5)	2.297(4)

Table 2 (Continued)

Complex **4**

O(12)−Nd(1)−O(24)	82.06(16)	O(24)−Nd(1)−O(28)	137.60(14)	O(15)−Nd(1)−O(26)	141.85(14)
O(12)−Nd(1)−O(22)	74.59(14)	O(15)−Nd(1)−O(28)	72.90(12)	O(22)−Nd(1)−O(23)	68.23(14)
O(24)−Nd(1)−O(15)	131.67(14)	O(27)−Nd(1)−O(28)	70.55(15)	O(15)−Nd(1)−O(23)	136.19(14)
O(22)−Nd(1)−O(15)	74.93(14)	O(12)−Nd(1)−O(26)	136.18(15)	O(12)−Nd(1)−O(25)	67.61(16)
O(15)−Nd(1)−O(27)	86.28(16)	O(24)−Nd(1)−O(26)	76.68(14)	O(24)−Nd(1)−O(25)	67.27(14)
O(12)−Nd(1)−O(28)	140.34(14)	O(22)−Nd(1)−O(26)	98.64(14)	O(22)−Nd(1)−O(25)	128.11(15)
O(13)−V(1)−O(5)	102.96(17)	O(14)−V(2)−O(7)	102.94(19)	O(21)−V(3)−O(19)	102.62(18)
O(5)−V(1)−O(1)	87.80(14)	O(14)−V(2)−O(11)	96.72(19)	O(21)−V(3)−O(16)	96.02(17)
O(1)−V(1)−O(3)	93.09(14)	O(7)−V(2)−O(11)	159.63(15)	O(19)−V(3)−O(16)	160.47(15)
O(13)−V(1)−N(2)	101.45(17)	O(9)−V(2)−O(11)	93.01(15)	O(17)−V(3)−O(16)	92.13(15)
O(3)−V(1)−N(2)	90.04(14)	O(14)−V(2)−N(3)	100.88(17)	O(21)−V(3)−N(6)	101.18(18)
O(13)−V(1)−N(1)	173.26(17)	O(11)−V(2)−N(3)	90.14(15)	O(16)−V(3)−N(6)	90.20(15)
O(5)−V(1)−N(1)	83.78(14)	O(14)−V(2)−N(4)	173.39(19)	O(21)−V(3)−N(5)	171.97(17)
O(1)−V(1)−N(1)	74.79(14)	O(7)−V(2)−N(4)	83.66(15)	O(19)−V(3)−N(5)	85.40(15)
N(2)−V(1)−N(1)	79.83(14)	N(3)−V(2)−N(4)	80.25(14)	N(6)−V(3)−N(5)	80.47(15)

[a] Symmetry transformations used to generate equivalent atoms: A $-x, -y, -z+1$ B $-x, -y+1, -z+1$ for **1**; A $-x+2, -y+1, -z+1$ B $-x+2, -y+1, -z$ for **2**; A $-x+3/2, -y+3/2, -z$ for **3** and **4**.

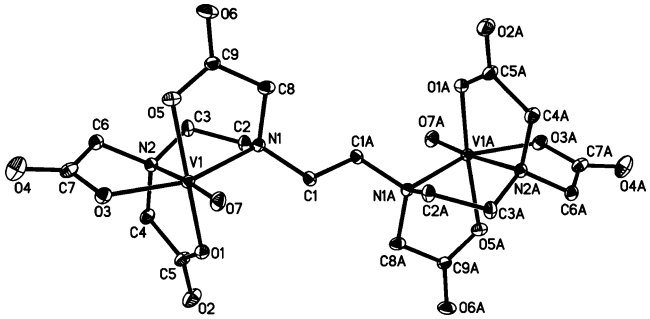

Figure 1. ORTEP drawing of the binuclear $[(VO)_2(TTHA)]^{2-}$ unit in **1** at 30% probability. H atoms were omitted for clarity.

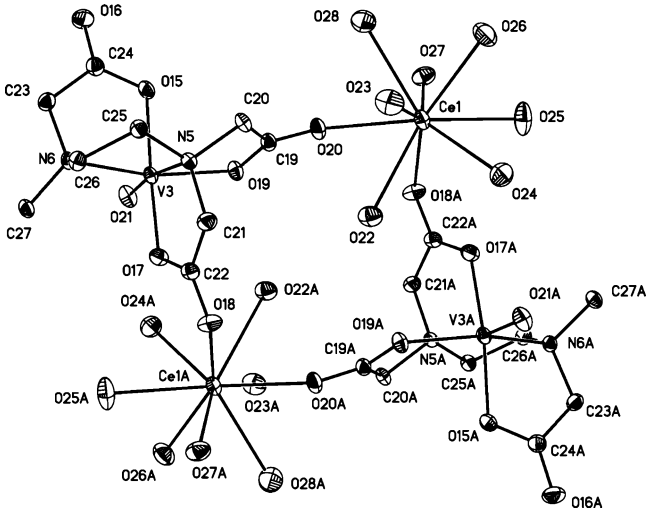

Figure 2. ORTEP drawing of Ce_2V_2 heterometallic square lattic and the coordination environment of Ce^{3+} and V^{4+} centers at 30% probability. H atoms were omitted for clarity.

mean equatorial plane toward the vanadyl oxygen atom by 0.396(1) Å. The V−N distances are clearly in the range of a typical V−N single bond,[17] of which the V1−N2 bond length (2.278(3) Å) has undergone a modest elongation due to the trans labilizing influence of the terminal oxo group as observed in other oxovanadium complexes.[18] In the binuclear $[(VO)_2(TTHA)]^{2-}$ unit, the V═O bonds are cis to the bridge but trans to each other. The V−O distance of 1.610(2) Åcompares well with the reported mean value of the V═O double bonds of 1.600(1) Å.[19] The V···V distance is 7.498-(7) Å.

Complex **2** crystallizes in a triclinic space group $P\bar{1}$ comprising a 1D chain structure of $[Ce(H_2O)_7(VO)(TTHA)_{0.5}]_n$ and the counterion of $[(VO)_2(TTHA)]^{2-}$. The Ce^{3+} and the V^{4+} centers are nine and six coordinated, respectively. Two oxygen atoms from two carboxylic groups, and seven oxygen atoms from coordinated water molecules complete the coordination sphere of the Ce^{3+} ion, which lies in a monocapped square-antiprism coordination environment. The average Ce−O bond length is 2.544(3) Å. The coordination geometries around the V^{4+} center of both the 1D chain and the counterion are pseudo-octahedral, which is similar to that of **1**. The vanadyl bond length varies from 1.592(3) to 1.600-(3) Å and compares well with the average value of 1.600(1) Å.[19] The Ce^{3+} and V^{4+} centers were alternately arrayed and linked by carboxyl groups of the TTHA anion to construct a heterometallic square lattice Ce_2V_2 with dimensions of 5.125 Å × 6.403 Å (Figure 2). This lattice composed of 3d−4f mixed metals was extremely rare, and further assembled into an infinite 1D chain linked through the −NCCN− bridges of TTHA (Figure 3). The V···V distance is 7.383(7) Å in the chain and 7.476(7) Å in the counterion, comparatively shorter than 7.498(7) Å of **1**. Another interest was given to the lattice water of this complex. There are two types of water molecules in the crystal lattice. One is discrete water molecules, while the other is the dimer of $(H_2O)_2$ (O31···O35, 2.790(3) Å and O32···O33, 2.760(3) Å) which were connected by strong hydrogen bonds with the bond lengths appropriate to the reported data.[20] The 1D chains and the counterions were connected by the water molecules through hydrogen bonds, forming a 3D supramolecular network.

(17) Yang, W.; Lu, C. *Inorg. Chem.* **2002**, *41*, 5638.
(18) Vergopoulos, V.; Priebsch, W.; Fritzsche, M.; Rehder, D. *Inorg. Chem.* **1993**, *32*, 1844.
(19) del Río, D.; Galindo, A.; Vicente, R.; Mealli, C.; Ienco, A.; Masi, D. *J. Chem. Soc., Dalton Trans.* **2003**, 1813.
(20) Cheruzel, L. E.; Pometun, M. S.; Cecil, M. R.; Mashuta, M. S.; Wittebort, R. J.; Buchanan, R. M. *Angew. Chem., Int. Ed.* **2003**, *42*, 5452.

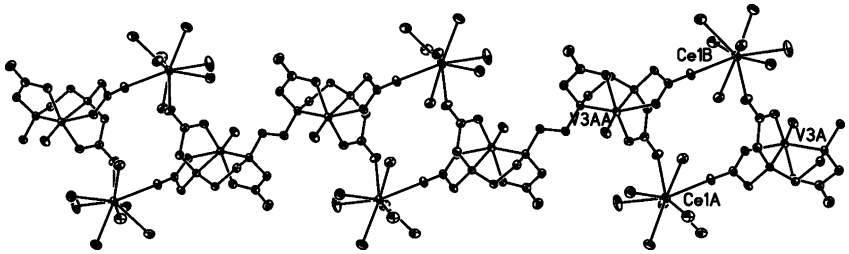

Figure 3. ORTEP drawing of the 1D chain of **2** at 30% probability. H atoms were omitted for clarity.

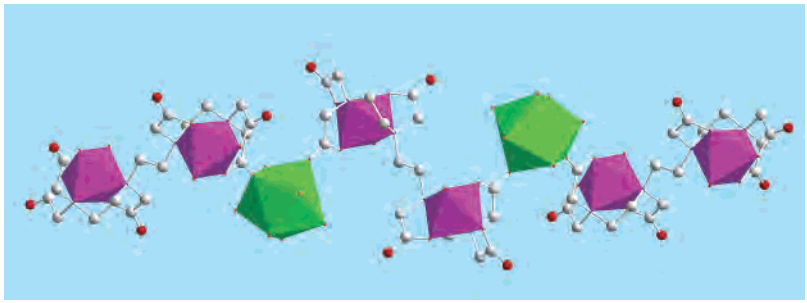

Figure 4. Molecular structure of octanuclear $[Pr_2(H_2O)_{14}(VO)_6(TTHA)_3]$ of **3**. H atoms were omitted for clarity. V, purple; Pr, green; O, red; C, white; N, blue.

Complexes **3** and **4** are isomorphic; both crystallized in monoclinic space group *C*2/*c*. Here complex **3** is taken as an example to depict the structure. The $[(VO)_2(TTHA)]^{2-}$ anion are almost the same as that in **1**. The Pr^{3+} ion lies in a little distorted monocapped square-antiprism coordination environment. Two oxygen atoms from two carboxylic groups of the $TTHA^{6-}$ anion and seven oxygen atoms from coordinated water molecules complete the coordination sphere. The average Pr−O bond length is 2.506(3) Å. Two Pr^{3+} cations linked three $[(VO)_2(TTHA)]^{2-}$ anions in an alternative way, forming an irregular linear octanuclear mixed-metal complex (Figure 4). The distance of the nearby Pr and V centers of the middle $[(VO)_2(TTHA)]^{2-}$ unit is 5.961(6) Å, while that of the terminal $[(VO)_2(TTHA)]^{2-}$ unit is 6.408(7) Å. The V···V distance is 7.382(7) Å in the middle unit and 7.466(7) Å in the terminal unit, also comparatively shorter than 7.498(7) Å of **1**. The linear octanuclear complex is very unusual in the literature, while this kind of mixed metals example is rather rare. In complex **4**, the Nd atoms take the place of Pr atoms. The decreasing atomic radius leads to the smaller average Nd−O bond length (2.491(3) Å) and V···Nd distance (5.940(5) and 6.387(6) Å). The water aggregations of linear $(H_2O)_4$ (O···O, 2.592(3)−3.181(4) Å) appeared in the crystal lattice which was different from **2** and also helps to form a 3D supramolecular network by hydrogen bonds.

According to the lanthanide contraction, the radius of the Ln^{3+} ion decreases with the increasing atomic number. In the respect that lanthanide ions always have similar chemical behaviors, the radius of the Ln^{3+} ion may play an important role during the structure formation. Few previous reports about adjusting atomic size in the structure modulation are concerned with lanthanide-containing polymers.[12] By their masses, the lanthanide series can be divided into three groups: the lighter La−Pm (Group 1), the intermediate Sm−Dy (Group 2), and the heavier Ho−Lu (Group 3). On the basis of our early reported results,[5d] we guess the lanthanide ions in Group 1 should form isostructural complexes because the radius decreases less compared to the decreasing from Group 1 to Group 3. However, the results still show different structures. The average bridging Ln−O bond lengths are decreasing for complexes **2**−**4** correspondingly. The reason may be due to both the degressive sizes of the lanthanide ions and the flexibility of the H_6TTHA ligand.[21]

IR and UV−Vis Spectra. The FTIR spectra of complexes **1**−**4** are similar. The main bands are contributed from the water molecules, carboxylic groups, and the double bond of the VO^{2+} ion, respectively. For example, in **1**, a broad band (2900−3700 cm^{-1}) of the $\nu(H_2O)$ centered at ca. 3440 cm^{-1} was observed. A very strong band of the antisymmetry stretching of carboxylic group appears at 1622 cm^{-1}, and the symmetrical stretching band of carboxylic group appears at 1378 cm^{-1}. The difference between the ν_{as} and ν_s is 244 cm^{-1}, comparatively larger than 200 cm^{-1}, which indicates the monochelation of the carboxylic group to the metal ion.[22] It is in accord with the X-ray crystal analysis. The band that appeared at 950 cm^{-1} has been attributed to the ν(V═O) stretching.[23]

The UV−vis spectra of the complexes **1**−**4** were measured in both the solid state and DMSO solution at a concentration of 2×10^{-3} mol·dm^{-1}. They are similar, but the positions of the peaks are some different. In solid-state spectra, all of the four complexes exhibit strong peaks at ca. 264 nm and shoulder peaks at ca. 340 nm, which are assigned to the intraligand $\pi-\pi^*$ transitions and the charge-transfer transitions of the VO^{2+} chromophores, respectively. Two relatively stronger peaks centered at ca. 585 and 780 nm can be attributed to the $d_{xy} \rightarrow d_{z^2}$ and $d_{xy} \rightarrow d_{yz}, d_{zx}$ transitions of the V^{4+} ion in an environment close to distorted octahedron.[23]

(21) Moeller, T.*The Chemistry of the Lanthanides*; Pergamon Press: Oxford, 1973.
(22) Nakamoto, K. *Infrared and Raman spectra of inorganic and coordination compounds*, 4th ed.; Wiley Press: New York, 1986.
(23) Sakmoto, M.; Ohsaki, M.; Yamamoto, K.; Nakayama, Y.; Matsumoto, A.; Okawa, H. *Bull. Chem. Soc. Jpn.* **1992**, *65*, 2514.

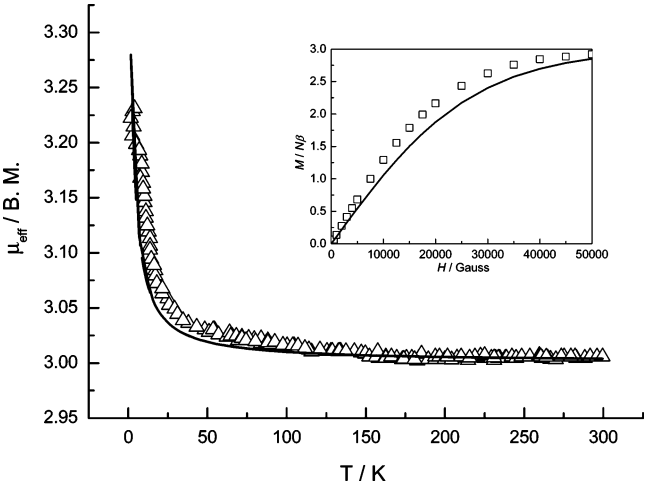

Figure 5. Plots of μ_{eff} vs T for **1** (△); the solid line represents the best fit. Inset: magnetization curve of **1** (□) at 2 K, solid line for three isolated VO^{2+} ions of Brillouin curve.

The transition of $d_{xy} \rightarrow d_{x^2-y^2}$ and the hypersensitive transition bands of the rare earth metal ions were not observed. In solution, the intraligand $\pi-\pi^*$ transitions were observed at ca. 260 nm. The d−d transitions appear at at ca. 592 and 780 nm. The f−f transitions was observed for Pr^{3+} ions of **3** at 448, 470 and 483 nm, which can be assigned to the $^3H_4 \rightarrow {}^3P_2$, $^3H_4 \rightarrow {}^3P_1$, and $^3H_4 \rightarrow {}^3P_0$ transitions, respectively. [24]

Magnetic Properties of 1. Great interest has been given to the magnetic properties of the complexes containing both transition and lanthanide metal ions. Owing to the simplest electronic configuration of V^{4+} (d^1), the V−Ln complexes were considered as an interesting family for the study of exchange coupling in 3d−4f complexes.[5a,d,e,25]

The magnetic susceptibilities of **1** were measured in the temperature range from 2 to 300 K. The room-temperature value of 3.01 μ_B for μ_{eff} is comparable to the value of 3.00 μ_B, that is, the spin-only value expected for three VO^{2+} ions with isotropic $g = 2.0$. As the temperature decreases, the value of μ_{eff} increases smoothly, and below 50 K it increases abruptly to the maximum of 3.23 μ_B at 2 K. This curve is in agreement with a ferromagnetic coupling between oxovanadium ions. The total magnetic susceptibility of χ_M is given by the sum of the contributions from the mononuclear cation $[VO(H_2O)_5]^{2+}$ and the binuclear anion $[(VO)_2(TTHA)]^{2-}$: $\chi_M = \chi_{Mono} + \chi_{Bi}$. χ_{Bi} was given by the expression of the Bleaney−Bowers type for binuclear $S = 1/2$ compounds based on the spin Hamiltonian $H = -2JS_1S_2$.[26] The result of the least-squares fit, shown as the solid line in Figure 5, was $g = 2.0$, $J = 1.98\ cm^{-1}$, $\theta = -0.14$ K, and $R = 7.8 \times 10^{-5}$ ($R = \sum(\chi_M^{obs} - \chi_M^{calc})^2/\sum(\chi_M^{obs})^2$). To confirm the ferromagnetic nature of the ground state, the field dependence of the magnetization, M, at 2 K was considered. The experimental $M-H$ curve (0−5 T, the inset in Figure 5) is higher than the Brillouin function for the sum of three isolated centers with $S = 1/2$ (solid line), which also supports the ferromagnetic interaction in **1**.

Scheme 1

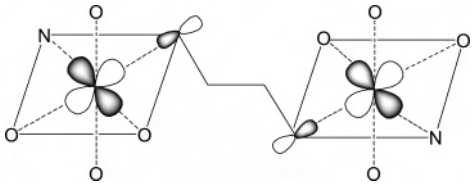

A qualitative interpretation of the magnetic interactions in transition metal dimers is usually given by the well-known Goodenough−Kanamori rules,[27] which are based on the interaction between pairs of natural magnetic orbital. The unpaired electron in oxovanadium(IV) complexes generally resides in a metal-centered orbital with d_{xy} character. According to Kahn's model, the exchange integral (J) can be decomposed into two terms, one ferromganetic (J_F) and the other antiferromagnetic contributions (J_{AF}).[28] The value of J_{AF} is proportional to the square of the integral overlap. In our case (Scheme 1), the value of overlap integral is close to zero (accidental orthogonality), which leads to ferromagnetic coupling.

Magnetic Properties of 2−4. Continuous interest was given to the magnetic behaviors of **2**−**4**. The magnetic susceptibilities were measured in the temperature range from 2 to 300 K. At room temperature, the μ_{eff} value of 4.10 μ_B of **2** is a little higher than the value of 3.93 μ_B, that is, the theoretical value for three isolated V^{4+} ions and one Ce^{3+} ion in the $^2F_{5/2}$ ground state ($g = 6/7$). Upon cooling, the μ_{eff} value slowly decreases to 3.85 μ_B at 16 K then decreases dramatically to 3.57 μ_B at 2 K. The total magnetic susceptibility of χ_M is offered from the sum of the contributions from the 1D chains of Ce−VO and the counterions of $[(VO)_2(TTHA)]^{2-}$. The magnetic behaviors of **3** and **4** are similar but different from **2.** For **3**, μ_{eff} value at room temperature is 4.69 μ_B, comparing well with the theoretical value of 4.67 μ_B, which is for three isolated V^{4+} ions and one Pr^{3+} ion in the $^3H_4$ ground state ($g = 4/5$). The μ_{eff} value decreases rapidly to 2.94 μ_B at 2 K upon cooling. For **4**, the room temperature μ_{eff} value of 4.47 μ_B is a little higher than the expected value of 4.37 μ_B for three isolated V^{4+} ions and one Nd^{3+} ion in the $^4I_{9/2}$ ground state ($g = 8/11$). Upon cooling, the μ_{eff} value decreases directly to 3.43 μ_B at 2 K.

The nature of magnetic coupling between adjacent V and Ln ions could not be interpreted exactly due to the large orbital angular momentum for lanthanide ions. The $4f^n$ configuration of Ln^{3+} is split into $^{2S+1}L_J$ spectroscopic levels by interelectronic repulsion and spin−orbit coupling. Each of these states is further split into Stark sublevels by the crystal field perturbation. At room temperature, all Stark sublevels are thermally populated. As the temperature is lowered, a depopulation of these sublevels occurs and, consequently, μ_{eff}^{Ln} decreases. When the Ln^{3+} interacts with

(24) Baker, A. T.; Hamer, A. M.; Livingstore, S. E. *Transition Met. Chem.* **1984**, *9*, 423.
(25) (a) Andruh, M.; Ramade, I.; Codjovi, E.; Guillou, O.; Kahn, O.; Trombe, J. C. *J. Am. Chem. Soc.* **1993**, *115*, 1822. (b) Benelli, C.; Blake, A. J.; Milne, P. E. Y.; Rawson, J. M.; Winpenny, R. E. P. *Chem. Eur. J.* **1995**, *1*, 614. (c) Costes, J. P.; Dahan, F.; Dupuis, A. *Inorg. Chem.* **2000**, *39*, 165.
(26) Bleaney, B.; Bowers, K. D. *Proc. R. Soc. London, Ser. A* **1952**, *266*, 95.
(27) Ginsberg, A. P. *Inorg. Chim. Acta Rev.* **1971**, *5*, 45.
(28) Kahn, O.; Charlot, M. F. *Nouv. J. Chim.* **1980**, *4*, 567.

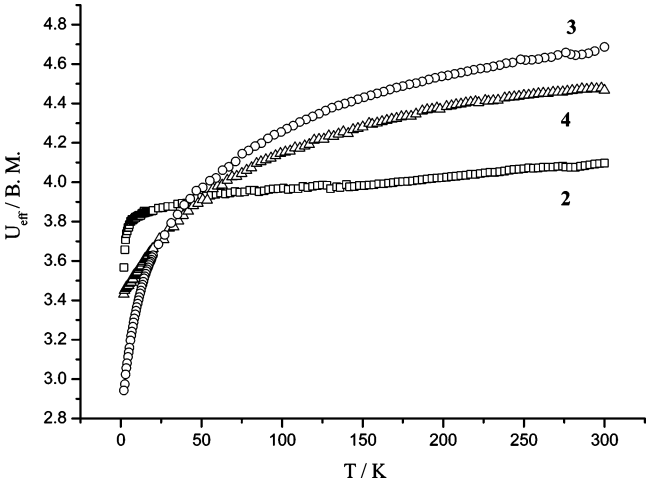

Figure 6. Plots of μ_{eff} vs T for **2**−**4**.

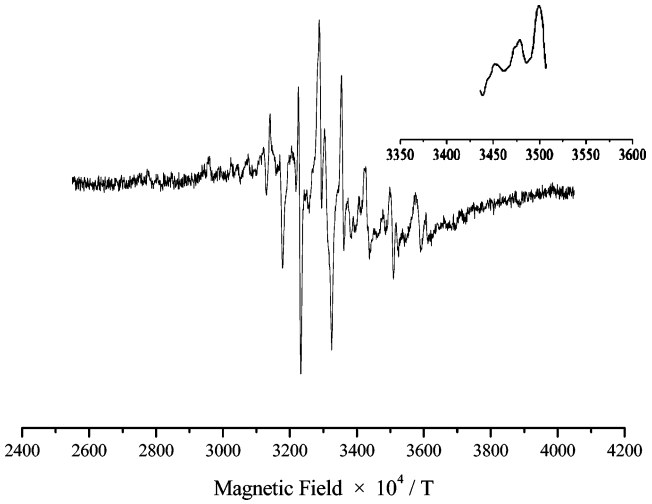

Figure 7. EPR spectrum of **1** recorded at 77 K in DMF solution. Inset: superhyperfine structure of nitrogen atoms.

another paramagnetic species, the temperature dependence of μ_{eff} is due to both the variation of $\mu_{eff}{}^{Ln}$ and the coupling between the Ln^{3+} and the second spin carrier. Thus, it is difficult to conclude that whether ferro- or antiferromagnetic interactions exhibit in complexes **2**−**4** only from the shape of the μ_{eff} versus T curve. As far as we know, there are two main methods to solve the problem: (a) To synthesize an isomorphic complex using a diamagnetic metal ion to take the place of the paramagnetic metal ion. By comparing the difference of μ_{eff} versus T curve of the two species, the nature of the magnetic interaction will appear;[29] (b) Using the Curie−Weiss law to estimate the magnetic interaction by the θ value, but it is not undoubted due to the complicated contributions to θ value. In these cases, the μ_{eff} versus T curve of **2** varies more smoothly comparing to the curves of **3** and **4**. The Curie−Weiss fits give the C value of 1.46, 2.98, and 2.64 emu K mol^{-1}, and θ value of 15.32, −30.31, and −22.71 K for **2**−**4** (in the temperature range 40−300 K), respectively. The results implied that there may be the

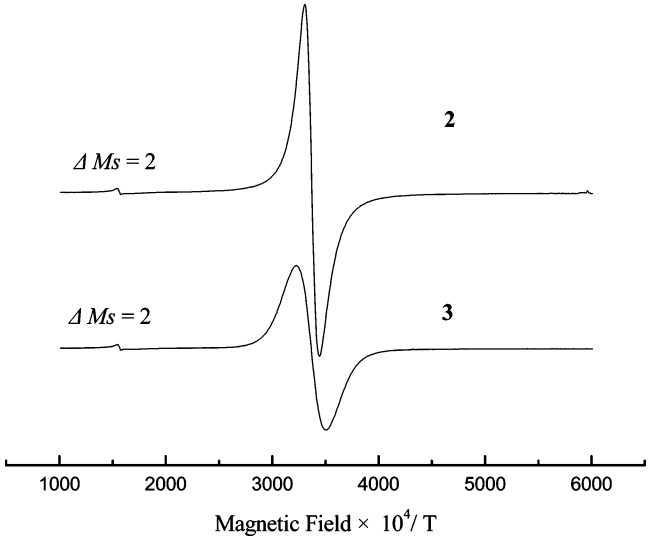

Figure 8. EPR spectrum of **2** and **3** recorded at 77 K in the solid state.

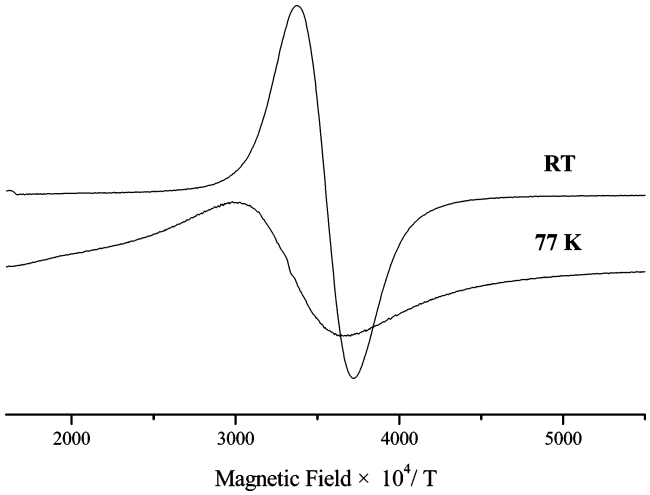

Figure 9. EPR spectrum of **4** recorded at room temperature and 77 K in the solid state.

ferromagnetic interaction in **2** and antiferromagnetic interactions in **3** and **4**.[30]

EPR Spectra. Since the vanadium(IV) ion has a simple $S = 1/2$ electronic spin, and ^{51}V has a high natural abundance of 99.75% and an $I = 7/2$ nuclear spin, the vanadyl ion can be used to assess the bonding of ligands to the divalent complex ion with characteristic signal. Though the EPR spectra of vanadium(IV) ion were well studied, systematic EPR investigation of a V−Ln system has been given little attention.

The X-band EPR powder spectra of **1** recorded at both room temperature and 77 K shows sharp bands centered at ca. $g = 1.97$ and 1.98, respectively. The signals at half field and the hyperfine pattern were not detected. In the frozen DMF solution, the hyperfine structure ($\langle A \rangle = 7.3$ mT, $\langle g \rangle = 2.0$) compares well with the mononuclear octahedral VO^{2+} complexes ($I = 7/2$).[31] The superhyperfine structure of nitrogen atoms is also found with the average A value of 2.5 mT (Figure 7).

(29) (a) Kahn, M. L.; Mathoniere, C.; Kahn, O. *Inorg. Chem.* **1999**, *38*, 3692. (b) Kahn, M. L.; Lecante, P.; Verelst, M.; Mathoniere, C.; Kahn, O. *Chem. Mater.* **2000**, *12*, 3073.

(30) Carlin, R. L. *Magnetochemistry*; Springer-Verlag: Berlin, 1986.

(31) (a) Wolff, F.; Lorber, C.; Choukroun, R.; Donnadieu, B. *Inorg. Chem.* **2003**, *42*, 7839. (b) Mukherjee, A.; Nethaji, M.; Chakravarty, A. R. *Chem. Commun.* **2003**, 2978.

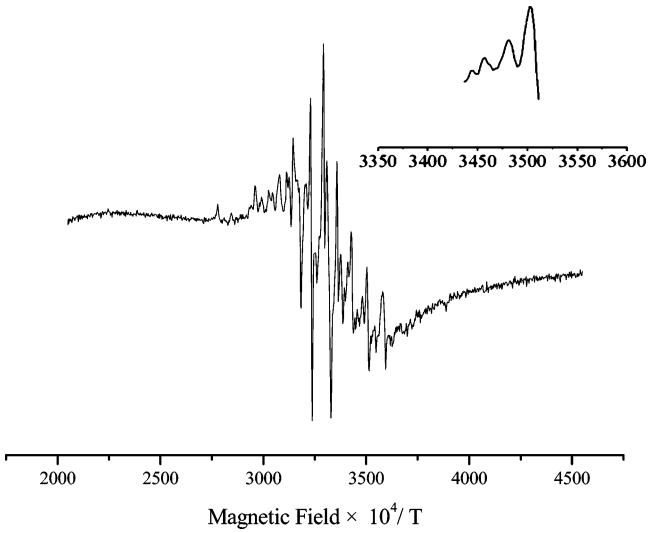

Figure 10. EPR spectrum of **4** recorded at 77 K in DMF solution. Inset: superhyperfine structure of nitrogen atoms.

The X-band EPR powder spectra of **2**−**4** recorded at both room temperature and 77 K show broad bands centered at ca. $g = 1.98$ except that **4** (77 K) centered at ca. $g = 2.03$, and no hyperfine pattern can be resolved. The spin-forbidden $\Delta M_s = 2$ transitions were observed for **2** and **3** (Figure 8). Abnormal line widths of **4** were observed upon temperature cooling. In normal EPR spectra, the line widths always became sharp when temperature decreases due to the concentration of the energy level with minor thermal perturbation. However, for **4**, the line width of 34.7 mT (calculated from the peak and trough of the first-order derive spectrum) at room temperature is lower than that of 66.9 mT in 77 K, which means the line width became wider (Figure 9). Considering relaxation and exchange interaction both narrow the line width when temperature cooling, this phenomenon maybe result from the dipole−dipole interaction of the Nd^{3+} ions in the complex.[30] This phenomenon was also observed in **2**, but with little variation (from 13.2 mT at room temperature to 14.2 mT at 77 K). In the frozen DMF solution at 77 K, unusual but similar hyperfine structures were observed for **2**−**4**. Figure 10 illustrates EPR spectrum of **4** with $\langle A \rangle = 7.1$ mT and $\langle g \rangle = 1.98$ as an example. Considering the interaction between vanadium atoms via the −NCCN− bridge in the binuclear units is comparatively weak, the hyperfine structure may be due to the magnetic spin-exchange interaction between the V^{4+} and Ln^{3+} ions. The superhyperfine structure of nitrogen atoms is also observed with the $\langle A \rangle$ value of 2.2 mT.

Conclusion

We have synthesized three new 3d−4f complexes based on a binuclear oxovanadium unit as SBUs. The results show that **1** is a useful ferromagnetic building block. Although the light lanthanide ions always exhibit similar chemical behavior, the structures of **2**−**4** are different. **2** is a 1D coordination polymer, comprising an unusual Ce_2V_2 heterometallic lattice in the chain structure. The isomorphic linear octanuclear structures of **3** and **4** seldom appeared in 3d−4f complexes were obtained. **2** is the second example of a oxovanadium(IV)−lanthanide(III) coordination polymer, and the heteronuclear linear complex is rather rare, which expands the realm of 3d−4f complexes. The investigations of the magnetic behavior of this system deserve further attention not only for the fundamental nature of vanadium-lanthanide complexes but also for understanding the chemistry of such compounds already in use and for future applications. Moreover, the successful synthesis of using the binuclear oxovanadium units as SBUs in this system provides an availably way of the construction of 3d−4f complexes.

Acknowledgment. This work was supported by the National Natural Science Foundation of China (Nos. 20425103 and 90501002) and the State Key Project of Fundamental Research of MOST (2005CCA01200), P. R. China.

Supporting Information Available: Crystallographic data in CIF format. This material is available free of charge via the Internet at http://pubs.acs.org.

IC051979Y